ARTICLE

The islet tissue plasminogen activator/plasmin system is upregulated with human islet amyloid polypeptide aggregation and protects beta cells from aggregation-induced toxicity

Nathalie Esser[1,2,3,4] · Meghan F. Hogan[1,2] · Andrew T. Templin[1,2,5] · Rehana Akter[1,2] · Brendy S. Fountaine[1] · Joseph J. Castillo[1,2] · Assam El-Osta[6] · Lakshan Manathunga[7,8] · Alexander Zhyvoloup[9] · Daniel P. Raleigh[7,8,9] · Sakeneh Zraika[1,2] · Rebecca L. Hull[1,2] · Steven E. Kahn[1,2]

Abstract

Aims/hypothesis Apart from its fibrinolytic activity, the tissue plasminogen activator (tPA)/plasmin system has been reported to cleave the peptide amyloid beta, attenuating brain amyloid deposition in Alzheimer's disease. As aggregation of human islet amyloid polypeptide (hIAPP) is toxic to beta cells, we sought to determine whether activation of the fibrinolytic system can also reduce islet amyloid deposition and its cytotoxic effects, which are both observed in type 2 diabetes.

Methods The expression of *Plat* (encoding tPA) and plasmin activity were measured in isolated islets from amyloid-prone hIAPP transgenic mice or non-transgenic control islets expressing non-amyloidogenic mouse islet amyloid polypeptide cultured in the absence or presence of the amyloid inhibitor Congo Red. *Plat* expression was also determined in hIAPP-treated primary islet endothelial cells, bone marrow-derived macrophages (BMDM) and INS-1 cells, in order to determine the islet cell type(s) producing tPA in response to hIAPP aggregation. Cell-free thioflavin-T assays and MS were used to respectively monitor hIAPP aggregation kinetics and investigate plasmin cleavage of hIAPP. Cell viability was assessed in INS-1 beta cells treated with hIAPP with or without plasmin. Finally, to confirm the findings in human samples, *PLAT* expression was measured in freshly isolated islets from donors with and without type 2 diabetes.

Results In isolated islets from transgenic mice, islet *Plat* expression and plasmin activity increased significantly with the process of amyloid deposition ($p \leq 0.01$, $n=5$); these effects were not observed in islets from non-transgenic mice and were blocked by Congo Red ($p \leq 0.01$, $n=4$). In response to hIAPP exposure, *Plat* expression increased in BMDM and INS-1 cells vs vehicle-treated cells ($p \leq 0.05$, $n=4$), but not in islet endothelial cells. Plasmin reduced hIAPP fibril formation in a dose-dependent manner in a cell-free system, and restored hIAPP-induced loss of cell viability in INS-1 beta cells ($p \leq 0.01$, $n=5$). Plasmin cleaved monomeric hIAPP, inducing a rapid decrease in the abundance of full-length hIAPP and the appearance of hIAPP 1–11 and 12–37 fragments. hIAPP 12–37, which contains the critical amyloidogenic region, was not toxic to INS-1 cells. Finally, *PLAT* expression was significantly increased by 2.4-fold in islets from donors with type 2 diabetes ($n=4$) vs islets from donors without type 2 diabetes ($n=7$) ($p \leq 0.05$).

Conclusions/interpretation The fibrinolytic system is upregulated in islets with hIAPP aggregation. Plasmin rapidly degrades hIAPP, limiting its aggregation into amyloid and thus protecting beta cells from hIAPP-induced toxicity. Thus, increasing islet plasmin activity might be a strategy to limit beta cell loss in type 2 diabetes.

Keywords Amyloid · Beta cell · Fibrinolysis · Human islet · Islet amyloid polypeptide · Plasmin · Tissue plasminogen activator · Type 2 diabetes

Abbreviations

Aβ	Amyloid beta
BMDM	Bone marrow-derived macrophages
Fmoc	9-Fluorenylmethylcarbonyl
hIAPP	Human islet amyloid polypeptide
IAPP	Islet amyloid polypeptide
M-CSF	Macrophage colony-stimulating factor
mIAPP	Mouse islet amyloid polypeptide
PAI-1	Plasminogen activator inhibitor-1
TFA	Trifluoroacetic acid
tPA	Tissue plasminogen activator
uPA	Urokinase plasminogen activator

Research in context

What is already known about this subject?

- Aggregation of the beta cell peptide human islet amyloid polypeptide (hIAPP) is toxic to beta cells

- The tissue plasminogen activator (tPA)/plasmin system is upregulated by brain amyloid deposition in Alzheimer's disease

- Plasmin cleaves peptides other than fibrin, including the amyloidogenic peptide amyloid beta

What is the key question?

- Is the tPA/plasmin system regulated by islet amyloid formation and can its upregulation reduce hIAPP aggregation and cytotoxicity?

What are the new findings?

- A local tPA/plasmin system is specifically upregulated in vitro in amyloid-laden mouse islets and is dependent on hIAPP aggregation. It is also upregulated in human islets from donors with type 2 diabetes vs donors without type 2 diabetes

- Plasmin is a hIAPP-degrading enzyme that protects beta cells from hIAPP-induced toxicity

- The hIAPP 1–11 and 12–37 fragments arising from plasmin-mediated cleavage of hIAPP are not toxic to beta cells

How might this impact on clinical practice in the foreseeable future?

- Increasing activity of the islet tPA/plasmin system might be a new strategy to reduce the deleterious impact of islet amyloid-induced beta cell toxicity in type 2 diabetes

Introduction

Type 2 diabetes is characterised by islet amyloid deposition, which is associated with beta cell loss and dysfunction [1–3]. Amyloid deposits contain the normal beta cell secretory product human islet amyloid polypeptide (hIAPP; also known as amylin) [4]. Since the process of hIAPP aggregation is toxic to beta cells [3, 5], the development of approaches to limit hIAPP aggregation could be beneficial for slowing or preventing beta cell loss in type 2 diabetes.

hIAPP is a 37 amino acid peptide, wherein the region comprising amino acids 20–29 plays an important role in dictating amyloidogenicity [6–8]. In contrast, due to several critical amino acid differences in this sequence and an H18R substitution, mouse islet amyloid polypeptide (mIAPP) is neither amyloidogenic nor cytotoxic [6]. Thus, transgenic mice expressing amyloidogenic hIAPP specifically in their beta cells have been produced to study islet amyloid formation. These mice develop amyloid deposits that are morphologically indistinguishable from those observed in human type 2 diabetes [9, 10] and have been used for both in vitro and in vivo studies of hIAPP aggregation and islet-amyloid-induced beta cell loss [9–12].

Based on bulk transcriptome analysis of amyloid-laden hIAPP mouse islets [13], we identified *Plat* as a gene specifically upregulated in islets under amyloid-forming conditions. *Plat* encodes tissue plasminogen activator (tPA), a secreted serine protease that initiates fibrinolysis by cleaving the circulating proenzyme plasminogen into the active protease plasmin, which, in turn, degrades fibrin blood clots [14]. In this process, fibrin is required for efficient tPA-mediated plasminogen activation [15]. Interestingly, both the amyloidogenic peptides hIAPP and amyloid beta (Aβ; the unique constituent of brain amyloid in Alzheimer's disease) can bind to tPA and substitute for fibrin in the tPA activation of plasminogen [16, 17]. Since the tPA/plasmin system has been reported to attenuate brain amyloid deposition by cleaving Aβ [18–20], we hypothesised that it may also be effective in reducing islet amyloid deposition and its cytotoxic effects in type 2 diabetes. In this study, we examined: (1) whether the tPA/plasmin system is upregulated in vitro in amyloid-laden mouse islets and in islets isolated from donors with type 2 diabetes; (2) the islet cell types expressing tPA; and (3) whether plasmin can limit hIAPP aggregation in a cell-free system and reduce hIAPP-induced beta cell toxicity.

Methods

Isolation and culture of mouse islets Transgenic mice with hemizygous expression of hIAPP under the rat insulin promotor (B6D2-Tg(RIP-hIAPP)CStka; generated as described in [21]) were bred on an F1 C57BL/6×DBA/2J background [10, 12]. Non-transgenic littermates were used as controls. Mice were housed and bred in a specific-pathogen-free vivarium at VA Puget Sound Health Care System, with ad libitum access to food and water. All animal studies described below were approved by the Institutional Animal Care and Use Committee at VA Puget Sound Health Care System, performed in an AAALAC-accredited animal research facility, and adhered to the Animal Research: Reporting of In Vivo Experiments guidelines.

Islets from 8–12 week-old male and female mice were isolated by collagenase digestion, as previously described [12]. Islets were handpicked and cultured overnight in complete RPMI-1640 medium containing 10% (vol./vol.) FBS, 1 mmol/l sodium pyruvate, 100 U/ml penicillin, 100 μg/ml streptomycin and 11.1 mmol/l glucose (complete medium). Thereafter, islets were distributed via a block randomisation method into islet pools and cultured for up to 144 h in complete RPMI medium containing either 11.1 mmol/l or 16.7 mmol/l glucose, the latter to induce amyloid deposition in hIAPP islets. The culture medium was renewed every 48 h. Subsets of islets were cultured for 48 h in the presence of Congo Red (200 μmol/l) or its vehicle control (DMSO), as done previously [22]. At the end of each experimental culture period, islets were collected for RNA extraction, plasmin activity measurement and/or histology, as described below.

For islet macrophage depletion, freshly isolated islets were cultured for 48 h in complete RPMI medium with 1 mg/ml clodronate-containing liposomes (Liposoma, Amsterdam, the Netherlands), or 1 mg/ml PBS-containing liposomes (Liposoma) or PBS alone as controls. Thereafter, they were transferred into complete RPMI medium containing 16.7 mmol/l glucose and cultured for 48 h, with the goal of inducing amyloid deposition in hIAPP transgenic islets. Subsequently, islets were collected for RNA extraction.

Islet plasmin activity assay Plasmin enzymatic activity in islet protein lysates was assayed by measuring the release of para-nitroaniline from the chromogenic substrate of plasmin S-2251 (Molecular Innovation, MI, USA). Briefly, Glu-plasminogen (0.5 μmol/l in 50 mmol/l Tris-HCl+100 mmol/l NaCl, pH 7.4; Molecular Innovation) and then S-2251 (0.4 mmol/l) were added to islet lysate samples (10 μg protein/sample, in duplicate) and mixed. The subsequent colour change was quantified at 405 nm after 120 min of incubation at 37°C on a Beckman Coulter DTX880 plate reader (Beckman Coulter, CA, USA).

Histology and quantitative microscopy Islets were formalin-fixed, paraffin-embedded and sectioned (10 μm). Sections were labelled with anti-insulin antibody (1:2000; Sigma-Aldrich, USA; catalogue no. I2018; RRID:AB_260137), followed by Cy3-conjugated goat anti-mouse IgG (1:250; Jackson ImmunoResearch Labs, West Grove, PA, USA; catalogue no. 115-165-146; RRID:AB_2338690, USA) and counterstaining with thioflavin-S (0.5% [wt/vol.] in aqueous solution; Sigma-Aldrich) to visualise beta cells and amyloid deposits [12]. The anti-insulin antibody was selected based on extensive validation in house. Sections were blocked for 1 h in buffer containing 0.05 mol/l PBS, 0.2% (wt/vol.) Triton X-100 (Sigma-Aldrich), 0.01% (wt/vol.) sodium azide (Sigma-Aldrich), 1% (wt/vol.) BSA (Sigma-Aldrich) and 2% normal goat serum (Vector Laboratories, USA). Antibodies were diluted in buffer containing 0.05 mol/l PBS, 0.2% (wt/vol.) Triton X-100, 0.01% (wt/vol.) sodium azide and 1% (wt/vol.) BSA. Islet images were acquired and analysed using a custom semi-automated workflow (Nikon TiE wide field microscope and Nikon NIS Elements AR v5.02.01 software; Nikon, USA). Briefly, islets were identified based on insulin immunofluorescence from a large area (×2) scan, and multichannel images were acquired at ×20. From these images, thioflavin-S-positive areas were computed based on pre-set pixel-density thresholds, using an automated method based on our previous manual approach [12] and image post-processing to compute islet cross-sectional areas. Amyloid prevalence was defined as the number of amyloid-positive islets/total number of islets×100, and amyloid severity as amyloid area/islet area×100 [3, 9, 13]. A mean of 18.5±1.8 islets per condition were analysed. The observer was blinded to genotype and culture conditions.

Peptide synthesis and purification Full-length hIAPP, hIAPP 1–11 and hIAPP 12–37 were synthesised using 9-fluorenylmethylcarbonyl (Fmoc) chemistry on a 0.10 mmol scale with a CEM Liberty Blue peptide synthesiser (CEM, USA) [23]. Fmoc-PAL-PEG-PS resin (Agilent; 0.19 mmol/eq) was used for C-terminal amidation of full-length hIAPP and hIAPP 12–37. Peptides were cleaved from the resin using a trifluoroacetic acid (TFA)-based cleavage cocktail (92.5% [vol./vol.] TFA, 2.5% [vol./vol.] triisopropylsilane, 2.5% [vol./vol.] 3,6-dioxa-1,8-octanedithiol and 2.5% [vol./vol.] water). Crude peptides were dried and then dissolved in 20% acetic acid (4 mg/ml) followed by lyophilisation to improve their solubility. The Cys2 and Cys7 disulfide bridge was assembled by oxidising the crude peptide in 100% DMSO (10 mg/ml). Reverse-phase HPLC was used to purify

the peptides. A Higgins Analytical C18 preparative column (Higgins Analytical, USA), 25 mm×250 mm, was employed with a binary A-B gradient of water and acetonitrile with 0.1% (vol./vol.) TFA. The purified peptides were lyophilised and redissolved in 1,1,1,3,3,3-hexafluoroisopropanol and subjected to a second round of reverse-phase HPLC purification. Analytical HPLC was used to confirm peptide purity and matrix-assisted laser desorption ionisation time-of-flight MS was used to verify the expected mass. mIAPP was purchased from Amyloid Peptide LLC (Danbury, CT, USA).

For cell treatment, islet amyloid polypeptide (IAPP) peptides were resuspended in Tris-HCl buffer (20 mmol/l, pH 7.4) to a final concentration of 250 μmol/l and then, immediately prior to use, diluted into complete media at final concentrations of 0–60 μmol/l.

Thioflavin-T fluorescence assays Kinetics of amyloid formation were determined using solutions containing hIAPP 1–37 and/or hIAPP 1–11 and/or hIAPP 12–37, and thioflavin-T (32 μmol/l; catalogue no. T3516; Sigma), and Tris-HCl (20 mmol/l, pH 7.4) in the presence or absence of plasmin (0–4 μmol/l; Molecular Innovation) or tPA (8 nmol/l; Molecular Innovation). Samples were incubated in triplicate at 25°C or 37°C, with plate shaking every 10 min, for up to 72 h. Fluorescence was recorded every 10 min on a Beckman Coulter DTX880 plate reader using an excitation wavelength of 450 nm and an emission wavelength of 485 nm. Control reactions were carried out in the absence of hIAPP peptides.

Negative stain transmission electron microscopy Samples (15 μl) of material collected at the end of the thioflavin-T assays were blotted onto carbon-coated formvar 300 mesh copper grids (Electron Microscopy Sciences, USA). The same volume of 1% (wt/vol.) depleted uranyl acetate was used to stain each sample. Images were recorded at the Central Microscopy Imaging Center facility at Stony Brook University (Stony Brook, NY, USA).

MS Full-length hIAPP (20 μmol/l) was incubated with or without human recombinant plasmin (0.4 μmol/l and 4 μmol/l; Molecular Innovation) at 37°C for up to 8 h. Samples were analysed by LC/MS after the indicated incubation time on an LTQ-Orbitrap XL mass spectrometer (ThermoFisher, USA).

Beta cell line experiments The beta cell line INS-1 832/13 (RRID: CVCL_7226), originally provided by C. Wollheim (University of Geneva, Geneva, Switzerland) [24], which was negative for mycoplasma, was cultured in complete RPMI medium. In total, $15×10^3$ cells/well were plated in triplicate into a gelatin-coated 96-well plate and incubated until confluency, after which the medium was replaced with complete RPMI medium containing freshly dissolved hIAPP

peptides (0–60 μmol/l) or Tris-HCl buffer (20 mmol/l, pH 7.4), as a control. After a 24 h incubation, cell viability was assessed using the fluorescent CellTiter-Fluor viability assay (Promega, Madison, WI, USA). Absorbance of a blank sample (no cells) was used to determine assay background, which was subtracted from every experimental sample. Each sample was normalised to buffer-treated cells. In a subset of experiments, cells were collected for RNA extraction at the end of the 24 h incubation with hIAPP (20 μmol/l) or Tris-HCl buffer (20 mmol/l, pH 7.4), as control.

Bone marrow-derived macrophage experiments Femur marrow from 6 month-old male Sprague Dawley rats (Charles River Laboratories, USA; www.criver.com/products-services/find-model/cd-sd-igs-rat?region=3611) was differentiated for 6 days in RPMI+10% (vol./vol.) FBS and 25 ng/ml recombinant human macrophage colony-stimulating factor (M-CSF; ThermoFisher) to make bone marrow-derived macrophages (BMDM). BMDM were then lifted from tissue culture plates using ice-cold PBS with 2 mmol/l EDTA, washed, plated and cultured overnight in RPMI+10% (vol./vol.) FBS and 25 ng/ml M-CSF. Subsequently, the medium was replaced with RPMI+10% (vol./vol.) FBS. After 48 h, the medium was replaced with complete RPMI containing freshly dissolved IAPP peptide (10 μmol/l) or Tris-HCl buffer (20 mmol/l, pH 7.4), as control. BMDM were incubated for 24 h and then collected for RNA extraction.

Human islets Human islets from male and female donors with or without type 2 diabetes were obtained from the Integrated Islet Distribution Program. Characteristics of the donors are listed in the electronic supplementary material (ESM) Table 1 (human islets checklist). Sex of the donors was determined based on the medical history from the organ procurement organisation via the isolation centre. Freshly isolated shipped islets (25–50 per donor) were collected for RNA extraction. As the human islets were anonymised, their use was not considered human research by the institutional review board.

Gene expression analysis Total RNA was extracted from islets or cells using the High Pure RNA Isolation Kit (Roche, Basel, Switzerland), reverse-transcribed using the High-Capacity cDNA Reverse Transcription Kit (ThermoFisher) and then subjected to quantitative RT-PCR (qRT-PCR).

cDNA samples from primary islet endothelial cells isolated from Sprague Dawley rats (Charles River Laboratories, USA; www.criver.com/products-services/find-model/cd-sd-igs-rat?region=3611) and treated for 24 h with IAPP peptides (20 μmol/l) or Tris-HCl buffer (20 mmol/l, pH 7.4) were made available from a previous study [25]. All cDNA samples were analysed in triplicate using pre-validated

Taqman gene expression assays (Life Technology, Foster City, CA, USA), with specific probes listed in ESM Table 2. Expression of each gene was calculated using the $\Delta\Delta C_t$ method, with *Ppib* or 18S as housekeeping genes.

Statistical analyses Data are presented as mean±SEM. Numbers of experimental replications are represented by individual data points in figures. Mean data were compared among treatment groups by one-way ANOVA followed by Holm–Šidák's multiple comparisons tests. A two-tailed Student *t* test was used when two groups were compared. A *p* value ≤0.05 was considered statistically significant. All statistical analyses were performed using Prism 9 (GraphPad Software, San Diego, CA, USA).

Results

Islet *Plat* expression and plasmin activity increase under amyloid-forming conditions To validate the RNA-seq data identifying *Plat* as a gene specifically upregulated within islets upon amyloid deposition (2.7 log$_2$-fold; $p=6.76^{-56}$) [13], we measured its expression in islets from hIAPP transgenic and non-transgenic mice cultured for up to 144 h in 16.7 mmol/l glucose (amyloid-forming conditions) or 11.1 mmol/l glucose (control). As expected, amyloid deposition increased in a time-dependent manner only in hIAPP transgenic islets cultured at 16.7 mmol/l glucose (Fig. 1a,b; data not shown for the 11.1 mmol/l glucose culture condition). Islet *Plat* mRNA levels increased over time in hIAPP transgenic islets under amyloid-forming conditions, whereas this increase was not observed in hIAPP transgenic islets cultured under non-amyloidogenic conditions (11.1 mmol/l

glucose) or mIAPP islets cultured in 11.1 mmol/l or 16.7 mmol/l glucose (Fig. 1c). Further, during this 144 h time-course period, *Plat* expression in amyloid-laden hIAPP transgenic islets cultured in 16.7 mmol/l glucose was significantly upregulated by 2.8±0.3-fold ($p≤0.001$), 7.5±2.4-fold ($p≤0.001$) and 4.5±0.6-fold ($p≤0.001$) at 48 h, 96 h and 144 h, respectively, when compared with non-transgenic control islets cultured in 16.7 mmol/l glucose (Fig. 1c).

To determine whether islet expression and activity of other components of the fibrinolytic system were impacted by the process of amyloid deposition, hIAPP transgenic and non-transgenic islets were cultured for 48 h in 11.1 mmol/l or 16.7 mmol/l glucose. *Plat* was upregulated in transgenic islets cultured in 16.7 mmol/l glucose vs transgenic islets cultured in 11.1 mmol/l glucose and non-transgenic islets cultured in 16.7 mmol/l glucose (Fig. 2a). However, there was no change in islet expression of the other fibrinolysis activator, urokinase plasminogen activator (uPA; encoded by *Plau*; Fig. 2b), or plasminogen activator inhibitor-1 (PAI-1; encoded by *Serpine1*; an endogenous inhibitor of tPA and uPA; Fig. 2c). Plasmin activity was significantly increased in transgenic islets under amyloidogenic conditions (Fig. 2d). In hIAPP transgenic islets, plasmin activity was significantly correlated with mRNA levels of *Plat* (Fig. 2e) but not *Plau* (Fig. 2f), suggesting the hIAPP aggregation-induced increase in islet *Plat* expression was associated with increased activity of the fibrinolytic system. Of note, no significant correlation was observed between *Plat* mRNA levels and plasmin activity in non-transgenic islets cultured in 11.1 mmol/l and 16.7 mmol/l glucose ($r^2=0.0073$, $p=0.8145$), indicating that this was not an effect of glucose per se.
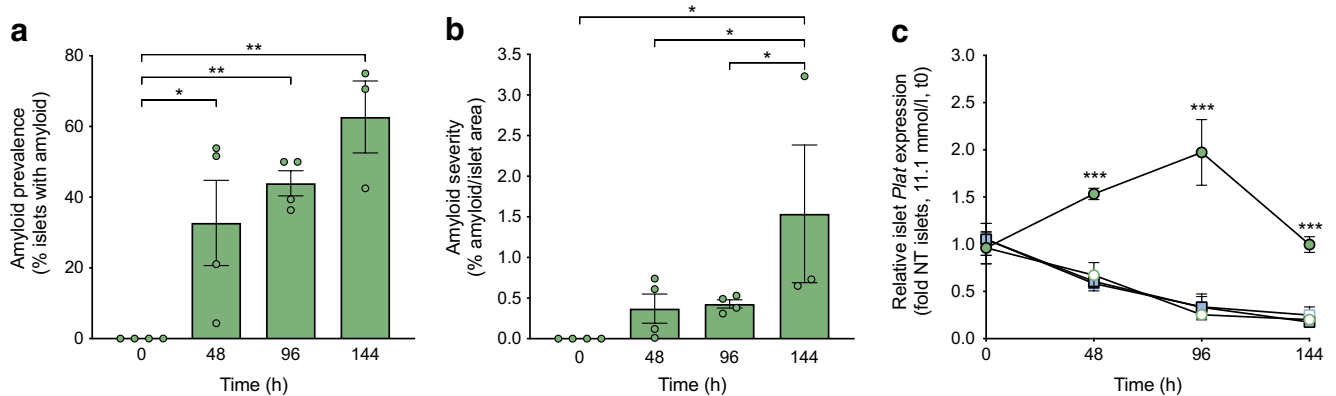

Fig. 1 Islet *Plat* expression increases with amyloid formation. (**a**, **b**) Time course of amyloid prevalence (% islets with amyloid; **a**) and severity (% amyloid/islet area; **b**) in hIAPP islets cultured at 16.7 mmol/l glucose. *n*=3–4; *$p≤0.05$, **$p≤0.01$. (**c**) Time course of *Plat* mRNA levels in hIAPP transgenic (green circles) and non-transgenic (NT; blue squares) islets cultured for up to 144 h in 11.1 mmol/l (open symbols) or 16.7 mmol/l (closed symbols) glucose conditions. Data are presented as fold expression relative to *Plat* expression in NT islets cultured in 11.1 mmol/l glucose at time 0. *n*=4; ***$p≤0.001$ for hIAPP islets cultured in 16.7 mmol/l glucose vs hIAPP islets cultured in 11.1 mmol/l glucose, or NT islets cultured in 16.7 mmol/l glucose or 11.1 mmol/l glucose, at the same time point
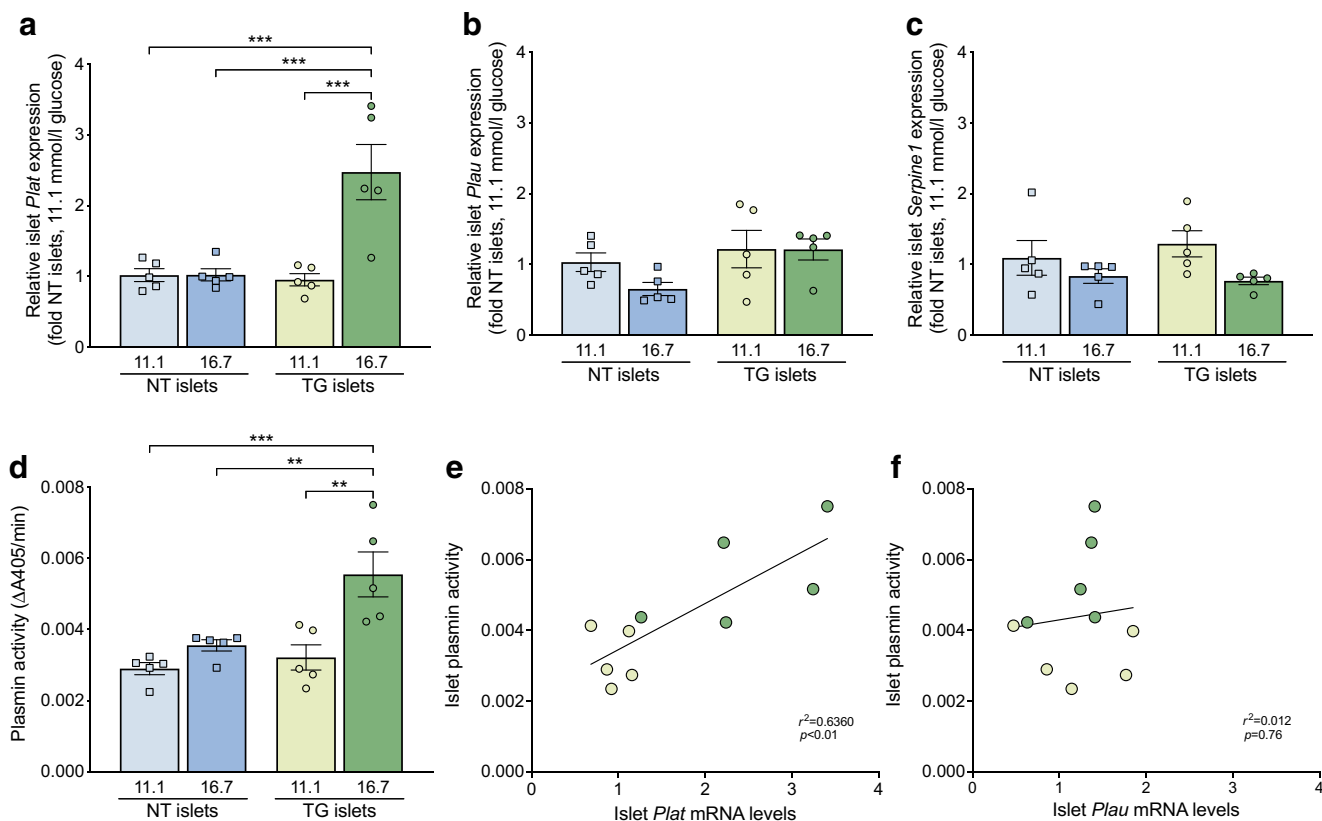
Fig. 2 Expression and activity of the components of the fibrinolytic system in islets under amyloid-forming conditions. (**a**–**c**) Quantification of *Plat* (**a**), *Plau* (**b**) and *Serpine1* (**c**) mRNA levels in non-transgenic (NT; blue squares) and hIAPP transgenic (TG; green circles) islets cultured for 48 h in 11.1 mmol/l or 16.7 mmol/l glucose conditions. Data are presented as fold expression relative to expression in NT islets cultured in 11.1 mmol/l glucose. (**d**) Islet plasmin activity in non-transgenic (NT; blue squares) and hIAPP transgenic (TG; green circles) islets cultured for 48 h in 11.1 mmol/l or 16.7 mmol/l glucose conditions. A405, absorbance at 405 nm. (**e**, **f**) Simple linear regression between islet plasmin activity and islet *Plat* (**e**) or *Plau* (**f**) mRNA levels in hIAPP transgenic islets cultured for 48 h in 11.1 mmol/l (light green circles) or 16.7 mmol/l (dark green circles) glucose conditions. $n=5$. **$p \leq 0.01$, ***$p \leq 0.001$

Islet *Plat* expression and plasmin activity are dependent on amyloid formation To evaluate whether the increase in islet *Plat* expression and plasmin activity depended on amyloid formation, hIAPP transgenic and non-transgenic islets were cultured for 48 h in 16.7 mmol/l glucose in the presence or absence of the amyloid inhibitor Congo Red. As expected, amyloid deposition was prevented in hIAPP islets in the presence of Congo Red (Fig. 3a). In parallel, increases in *Plat* expression (Fig. 3b) and plasmin activity (Fig. 3c) in hIAPP transgenic islets were abrogated with Congo Red, while Congo Red had no effect in non-transgenic islets. These findings imply that the increase in *Plat* expression and plasmin activity was downstream of amyloid formation.

hIAPP increases *Plat* expression in macrophages and beta cells but not endothelial cells We next sought to investigate the islet cell type(s) in which tPA is increased in response to hIAPP aggregation. As endothelial cells are characterised as the major tPA-producing cell type [26] and have been described to be targets of toxic and/or inflammatory effects

of amyloid formation [25], we first determined whether hIAPP treatment stimulates *Plat* expression in these cells. Primary rat islet endothelial cells were treated for 24 h with hIAPP, non-amyloidogenic mIAPP, or vehicle, as control. Treatment with 20 μmol/l hIAPP (which we have previously shown to decrease cell viability and increase expression of endothelial cell activation markers [25]) did not increase *Plat* expression in these cells (Fig. 4a).

Since macrophages also produce tPA [27] and can be activated by hIAPP (10 μmol/l) [28, 29], we determined whether hIAPP increases *Plat* expression in these cells. *Plat* mRNA levels were quantified in rat BMDM treated for 24 h with hIAPP, mIAPP or vehicle. *Plat* expression significantly increased by fourfold solely with hIAPP treatment (Fig. 4b). Interestingly, hIAPP was also effective at increasing *Plat* expression in INS-1 beta cells (Fig. 4c), suggesting macrophages may not be the sole source of the hIAPP-induced increase in tPA in the islet.

To further determine the contribution of islet macrophages to tPA upregulation by hIAPP aggregation,
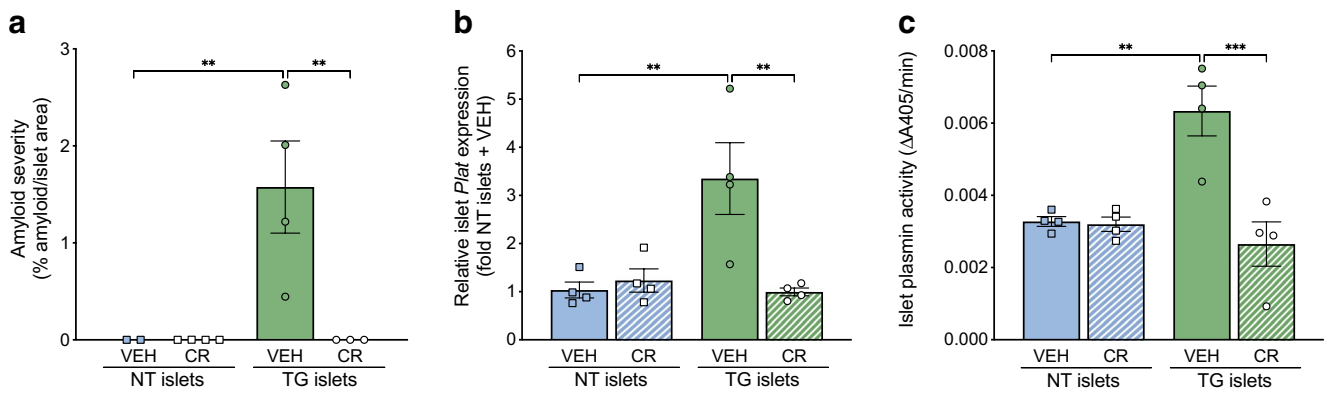
Fig. 3 Islet *Plat* expression and plasmin activity are dependent on amyloid formation. (**a**–**c**) Amyloid formation (**a**), *Plat* mRNA levels (presented as fold expression relative to expression in non-transgenic [NT] islets cultured in 16.7 mmol/l glucose with vehicle [VEH]) (**b**) and plasmin activity (**c**) in NT and hIAPP transgenic (TG) islets cul-tured for 48 h in 16.7 mmol/l glucose conditions in the presence of the known amyloid inhibitor Congo Red (CR; 200 μmol/l) or its VEH (DMSO) control. A405, absorbance at 405 nm. n=2–4. **p≤0.01, ***p≤0.001
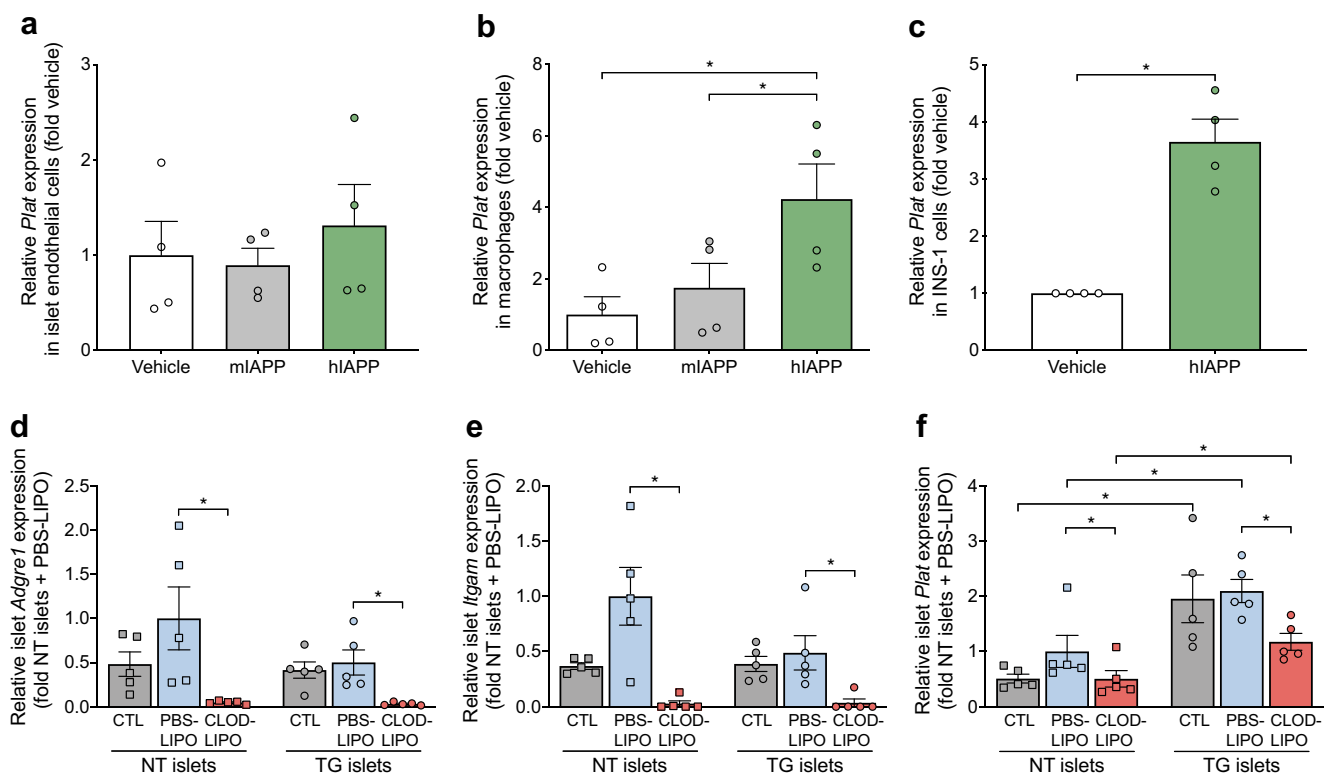
Fig. 4 Islet cell types producing tPA in response to hIAPP aggrega-tion. (**a**–**c**) Quantification of *Plat* mRNA levels in primary rat islet endothelial cells (**a**), rat BMDM (**b**) and INS-1 cells (an immortal-ised beta cell line) (**c**) treated for 24 h with hIAPP (20 μmol/l), or the non-amyloidogenic mIAPP (20 μmol/l) or vehicle (Tris-HCl buffer) as controls. Data are presented as fold expression relative to expres-sion in cells treated with vehicle. n=4 independent experiments for each cell type. (**d**–**f**) Quantification of *Adgre1* (**d**), *Itgam* (**e**) and *Plat* (**f**) mRNA levels in hIAPP transgenic (TG) and non-transgenic (NT) islets treated for 48 h with clodronate-containing liposomes (CLOD-LIPO), PBS-containing liposomes (PBS-LIPO) or PBS alone (CTL), and then cultured for 48 h in 16.7 mmol/l glucose conditions. Data are presented as fold expression relative to expression in NT islets treated with PBS-LIPO and then cultured in 16.7 mmol/l glucose. n=5. *p≤0.05

isolated hIAPP transgenic and non-transgenic islets were treated with clodronate-containing liposomes to deplete macrophages, or PBS-containing liposomes or PBS alone as controls. Islets were then cultured for 48 h in 16.7 mmol/l glucose to induce amyloid deposition in hIAPP islets, after which islet macrophage markers (*Adgre1* and *Itgam*) and *Plat* mRNA levels were quantified. In both hIAPP transgenic and non-transgenic islets, clodronate treatment significantly abrogated *Adgre1* (Fig. 4d) and *Itgam* (Fig. 4e) expression compared with controls treated with PBS-containing liposome, confirming islet macrophage depletion in both genotypes. As expected, *Plat* expression significantly increased by 2.1-fold in hIAPP islets treated with PBS-containing liposomes vs non-transgenic islets treated the same (Fig. 4f). Clodronate treatment also significantly reduced *Plat* expression (vs islets treated with PBS-containing liposomes) in both hIAPP and non-transgenic islets; however, *Plat* expression was still increased by 2.3-fold in

clodronate-containing-liposome-treated hIAPP islets vs non-transgenic islets treated the same (Fig. 4f). These data suggest that, in addition to macrophages, other islet cell types (e.g. beta cells) produce tPA in response to hIAPP aggregation.

Plasmin protects beta cells from hIAPP-induced cytotoxicity by cleaving hIAPP and inhibiting fibril formation Given that plasmin degrades the amyloidogenic peptide Aβ [18], we next sought to determine whether plasmin also cleaves hIAPP and could, thereby, prevent its aggregation. Using thioflavin-T assays, we found that plasmin decreases hIAPP fibril formation in a dose-dependent manner (ESM Fig. 1), with 0.4 μmol/l plasmin abrogating fibril formation by 95.6% (Fig. 5a,b). In contrast, tPA alone had no measurable effect on hIAPP fibril formation (ESM Fig. 1). Furthermore, treatment of the beta cell line INS-1 for 24 h with hIAPP in the presence or absence of plasmin showed that
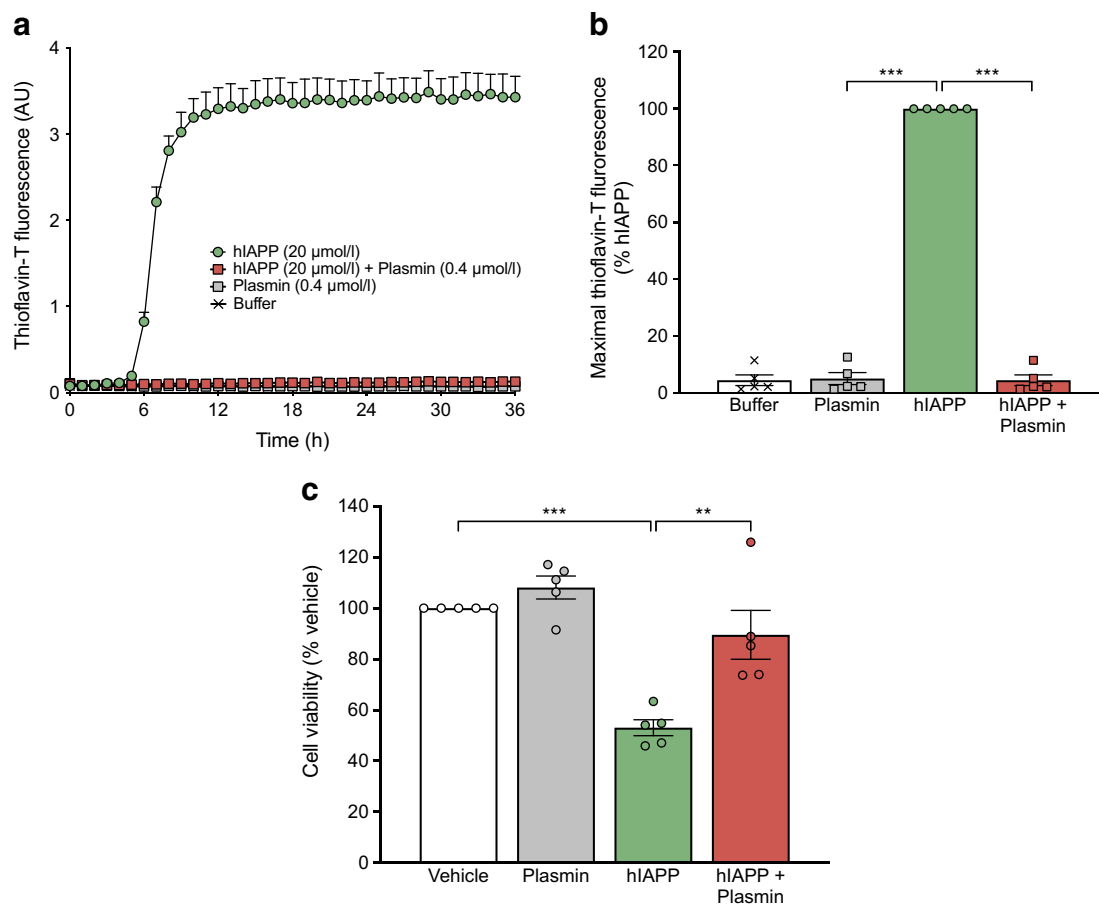

Fig. 5 Plasmin reduces hIAPP fibril formation and protects beta cells from hIAPP-induced cytotoxicity. (**a**) Amyloid formation assays of hIAPP (20 μmol/l) carried out in the absence or presence of plasmin (0.4 μmol/l) and monitored for 36 h at 37°C by thioflavin-T fluorescence in a cell-free system. 'Buffer' is Tris-HCl (20 mmol/l, pH 7.4). One representative experiment is shown with technical triplicates.

AU, arbitrary units. (**b**) Quantification of maximal hIAPP aggregation with hIAPP (20 μmol/l) and/or plasmin (0.4 μmol/l). 'Buffer' is Tris-HCl (20 mmol/l, pH 7.4). *n*=5. (**c**) Cell viability (CellTiter-Fluor [CTF] assay) of INS-1 cells treated for 24 h with vehicle (Tris-HCl), hIAPP (20 μmol/l) and/or plasmin (0.4 μmol/l). *n*=5. ****p≤0.01, ***p≤0.001**

plasmin prevented hIAPP-induced decreases in cell viability (Fig. 5c).

Using MS, we found that plasmin cleaves monomeric hIAPP generating hIAPP 1–11 and 12–37 fragments. Incubation of hIAPP with plasmin followed by LC/MS analysis of these cleavage products as a function of time showed that plasmin induces a rapid decrease in the abundance of full-length hIAPP and the appearance of the 1–11 and 12–37 fragments (Fig. 6a), confirming that plasmin cleaves monomeric hIAPP between amino acid 11 and 12 (Fig. 6b).

hIAPP 12–37 forms amyloid more rapidly than full-length hIAPP, but is not cytotoxic We next assessed the amyloidogenicity and cytotoxicity of hIAPP 1–11 and 12–37. Using thioflavin-T assays, we found that hIAPP 1–11 did not aggregate (Fig. 7a) whereas hIAPP 12–37 aggregated faster than full-length hIAPP (Fig. 7b). While the kinetics of full-length hIAPP aggregation showed a typical initial lag phase followed by a sigmoidal transition to a steady state [30], there was no visible lag phase during aggregation of hIAPP 12–37 (Fig. 7b). Maximal thioflavin-T fluorescence of the fragment was lower than the same concentration of full-length hIAPP ($p \leq 0.001$; $n=4$). By treating INS-1 cells for 24 h with increasing doses of hIAPP 12–37 or full-length hIAPP, we found that full-length hIAPP reduces cell viability in a dose-dependent manner, while, in contrast, hIAPP 12–37 was not cytotoxic to INS-1 cells, even at 60 μmol/l (Fig. 7c).

Some hIAPP-derived fragments have been shown to inhibit or enhance the aggregation kinetics of full-length hIAPP [11, 31]. Thus, mixtures of full-length hIAPP and 1–11 or 12–37 fragments were analysed to determine whether the fragments modulate amyloid formation by the full-length peptide. The addition of hIAPP 1–11 to hIAPP 1–37 did not alter the aggregation kinetics of full-length hIAPP (Fig. 7d). In concentration ratios of 0.5:1 to 2:1 of 12–37:full-length hIAPP, the mixture aggregated rapidly, indicating that hIAPP 12–37 accelerates aggregation of full-length hIAPP (Fig. 7e). By treating INS-1 cells for 24 h with mixtures of hIAPP 1–37 and the hIAPP fragments, we found that the addition of 1–11 and/or 12–37 fragments to full-length hIAPP did not reverse the 50% reduction in cell viability induced by full-length hIAPP (Fig. 7f). Further, addition of a high concentration (40 μmol/l) of the 12–37 fragment or mixtures of 1–11 and 12–37 fragments to hIAPP 1–37 led to mixtures that were more toxic to INS-1 cells than hIAPP 1–37 alone (Fig. 7f).

Thioflavin-T assays accurately report amyloid formation by wild-type hIAPP and a wide range of IAPP mutants; however, since the dye is an extrinsic probe, it was important to assess amyloid formation with an independent method [32]. Transmission electron microscopy imaging revealed that hIAPP 12–37 fibrils were similar in appearance to those formed by full-length hIAPP (Fig. 7g).

Taken together these data indicate that, by generating hIAPP fragments that alone or when combined with each other are not cytotoxic, plasmin-mediated cleavage of hIAPP may protect beta cells from hIAPP aggregation-induced cytotoxicity.

Islet *PLAT* and *SERPINE1* mRNA levels are increased in human type 2 diabetes To determine whether islet tPA is increased in type 2 diabetes, *PLAT* mRNA levels were measured in islets isolated from donors with and without type 2 diabetes. *PLAT* mRNA levels were increased by 2.4-fold in islets from donors with type 2 diabetes compared with control islets (Fig. 8a). Further, *SERPINE1* mRNA levels were also increased by 2.6-fold in islets from donors with type 2 diabetes compared with control islets (Fig. 8b). Both *PLAT* and *SERPINE1* genes were detectable in islets from male and female donors. Given the sex/gender distribution of human islets received from the organ procurement organisation, it was not possible to do formal analyses of any gender-/sex-based effect.
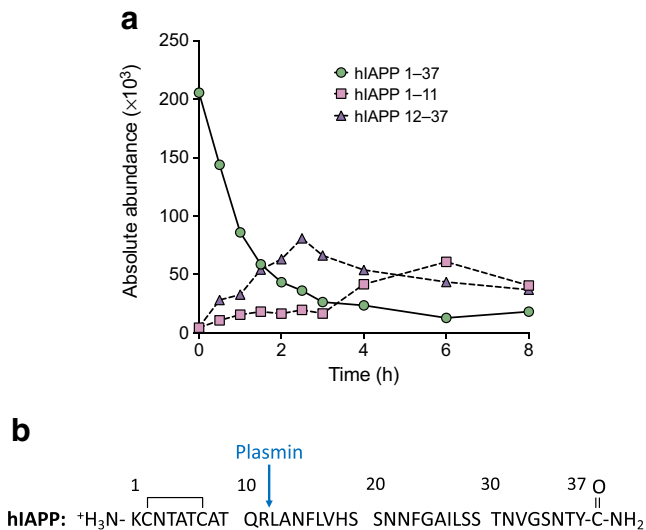
Fig. 6 Plasmin cleaves monomeric hIAPP between amino acids 11 and 12. (**a**) Abundance of full-length hIAPP (hIAPP 1–37), hIAPP 1–11 and hIAPP 12–37 measured by LC/MS at 0, 2, 4, 6 and 8 h after combining hIAPP (20 μmol/l) with human plasmin (0.4 μmol/l). (**b**) The primary sequence of hIAPP with the MS-identified site of plasmin cleavage is shown by the blue arrow

Discussion

Islet amyloid deposition, which occurs in the vast majority of people with type 2 diabetes, is associated with beta cell loss and secretory dysfunction, both of which critically contribute to the development of the disease [1–3]. In this study, we delineated a new intra-islet role for the fibrinolytic
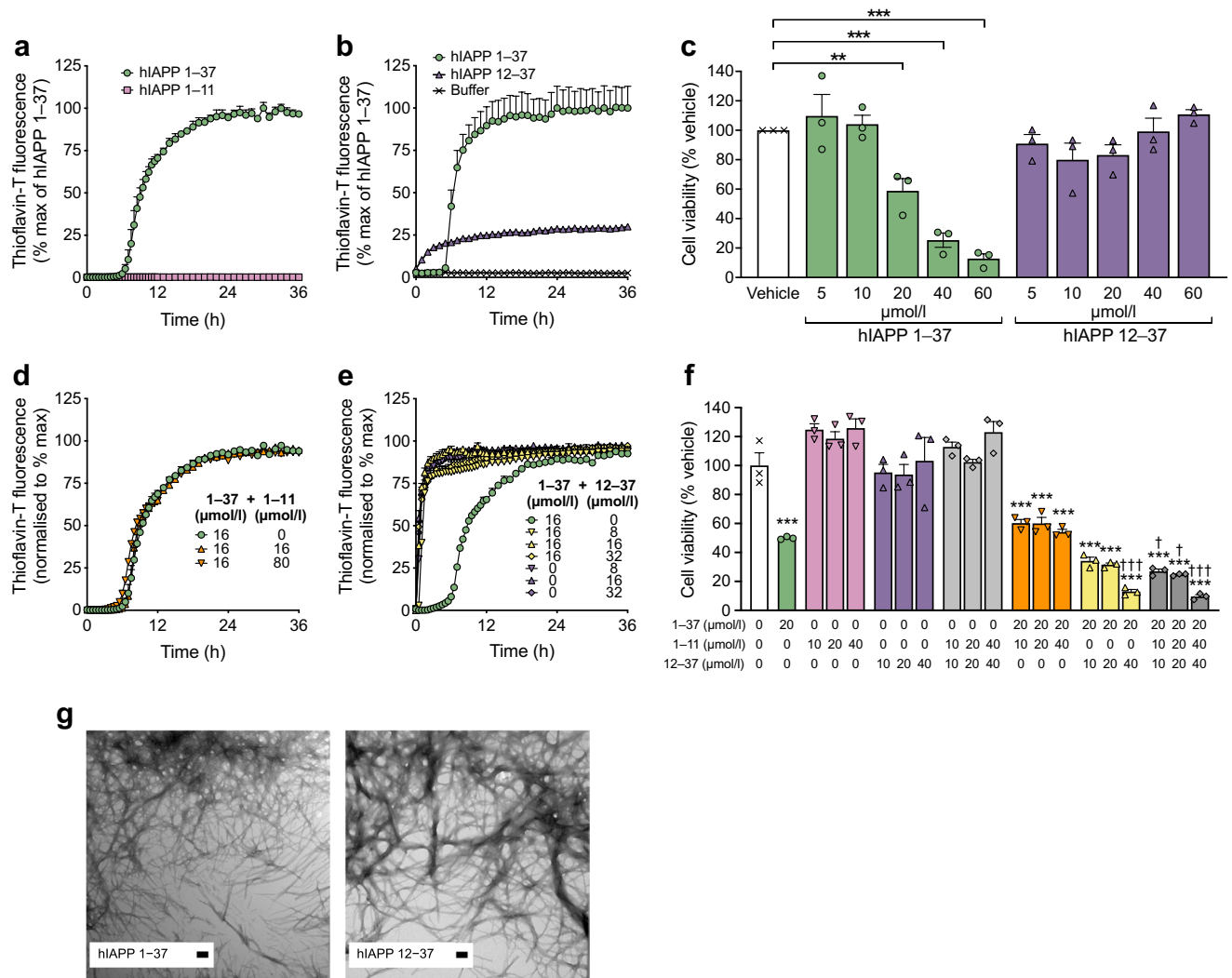
Fig. 7 hIAPP 12–37 is not cytotoxic, aggregates faster than hIAPP 1–37 and accelerates amyloid formation by hIAPP 1–37. (**a**, **b**) Thioflavin-T fluorescence profiles of amyloid formation kinetics for full-length hIAPP and the hIAPP 1–11 fragment (**a**), and full-length hIAPP, the hIAPP 12–37 fragment and buffer (Tris-HCl 20 mmol/l, pH 7.4) (**b**), monitored for 36 h at 37°C. In (**a**) and (**b**), one representative experiment is shown with technical triplicates. (**c**) Cell viability (CellTiter-Fluor [CTF] assay) of INS-1 cells treated for 24 h with vehicle or increasing concentrations of hIAPP 1–37 or hIAPP 12–37. $n=3$. $**p \leq 0.01$, $***p \leq 0.001$. (**d**, **e**) Thioflavin-T fluorescence profiles of amyloid formation kinetics for full-length hIAPP alone (16 µmol/l) or with the addition of hIAPP 1–11 in ratios of 1:1 and 1:5 (**d**), and full-length hIAPP alone (16 µmol/l) or with the addition of hIAPP 12–37 in ratios of 1:0.5, 1:1 and 1:2, or hIAPP 12–37 alone (**e**), monitored for 36 h at 25°C. In (**d**) and (**e**), one representative experiment is shown with technical triplicates. (**f**) Cell viability (CTF assay) of INS-1 cells treated for 24 h with vehicle (Tris-HCl, 20 mmol/l, pH 7.4), or hIAPP 1–37, 1–11 or 12–37 alone or combined in different ratios. $n=3$. $***p \leq 0.001$ vs vehicle; $†p \leq 0.05$, $†††p \leq 0.001$ vs hIAPP 1–37 alone. (**g**) Transmission electron microscopy-derived representative images of full-length hIAPP and hIAPP 12–37. Images were taken at the end of the kinetic reactions. Scale bar, 100 nm

system in modulating amyloidogenesis. We found islet *Plat* expression and plasmin activity to be specifically upregulated with the aggregation of hIAPP. Further, plasmin cleaved hIAPP, abrogated its aggregation and protected beta cells from hIAPP-induced toxicity. Our data also demonstrated that hIAPP aggregation increases *Plat* expression in islet macrophages and beta cells. Finally, *PLAT* expression was increased in islets from donors with type 2 diabetes.

Apart from its fibrinolytic activity, several studies have reported that the tPA/plasmin system may be involved in amyloidogenesis. Specifically, it has been demonstrated that the tPA/plasmin system is induced by Aβ aggregation in Alzheimer's disease and can reduce brain amyloid deposition [18–20]. In addition, it has been shown that tPA is able to bind to IAPP fibrils [16]. Moreover, aggregated hIAPP and Aβ can mediate tPA activation of plasminogen

Fig. 8 *PLAT* and *SERPINE1* genes are expressed in human islets and increased with type 2 diabetes. (**a**, **b**) Quantification of (**a**) *PLAT* and (**b**) *SERPINE1* mRNA levels in islets from male (M) and female (F) donors with (n=4; 1M/3F) or without (n=7; 6M/1F) type 2 diabetes. Data are normalised to 18S ribosomal RNA (rRNA) and expressed as fold relative to control. *$p \le 0.05$
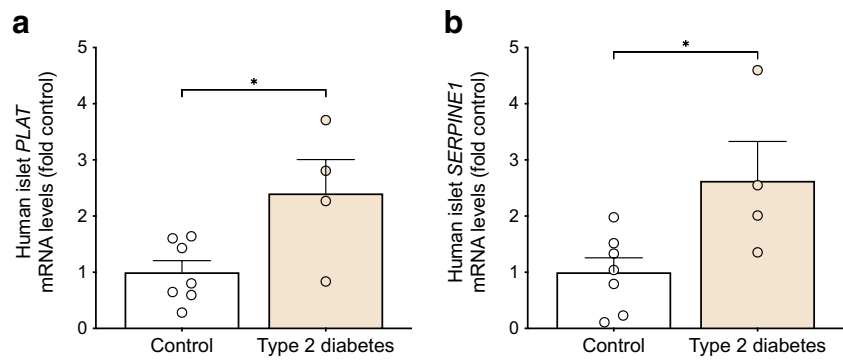
in the absence of fibrin [17]. Importantly, our study reinforces a role for the fibrinolytic system in amyloidogenesis by showing that the tPA/plasmin system is upregulated in amyloid-laden islets, and that plasmin reduces hIAPP aggregation and protects beta cells from hIAPP aggregation-induced toxicity. Since plasmin can also be generated from plasminogen through the proteolytic activities of uPA, we measured islet *Plau* expression and found it was not increased in amyloid-laden islets. Further, treatment of hIAPP islets with Congo Red blocked amyloid fibril formation and *Plat* upregulation, suggesting that modulation of *Plat* expression is downstream of amyloid formation. Future work determining the mechanism(s) by which this effect occurs in amyloid-laden islets will be of interest. For example, a potential area for future research may involve the interleukin-1 beta pathway since interleukin-1 beta has been shown to upregulate the tPA/plasmin system in mesangial cells [33], and we and others have demonstrated that hIAPP aggregation increases interleukin-1 beta production in islets [28, 29].

Importantly, we confirmed our findings in human islets, showing that *PLAT* expression is increased with type 2 diabetes. As aforementioned, given the sex/gender distribution of human islets received from the organ procurement organisation, we were unable to formally analyse gender-/sex-based effect. However, gender-/sex-based effects would not be expected given that islet amyloid occurs in both male and female individuals with type 2 diabetes [3]. Further, even though the expression of islet *Serpine1* (encoding PAI-1, the endogenous inhibitor of tPA and uPA) was not affected by amyloid deposition in rodent islets in vitro, we found its expression to be increased in islets from donors with type 2 diabetes. Of note, a previous study has identified PAI-1 as a novel glucose-regulated protein, elevated under high glucose conditions in cultured human islets [34]. These data suggest the tPA/plasmin system could act to reduce islet amyloid accumulation, and the increase in PAI-1 in type 2 diabetes could inhibit a physiological protective effect of the fibrinolytic system in the islet. We also cannot exclude the possibility that the increase in systemic PAI-1 levels and activity in

obesity and the metabolic syndrome may have a role in type 2 diabetes development [35–38].

Previous studies have shown that plasmin can degrade peptides other than fibrin, including the amyloidogenic peptide Aβ [18]. In this study we have identified plasmin as an hIAPP-degrading enzyme. Typically, plasmin-targeting cleavage sites are located after the basic amino acids lysine or arginine, but rare cleavages have also been described after histidine or glutamine [39]. Using MS, we found plasmin predominantly cleaves hIAPP at one of the predicted sites, the Arg-11-Leu-12 peptide bond, producing hIAPP 1–11 and 12–37 fragments. This is of importance since we and others have previously reported that several hIAPP-degrading enzymes, such as neprilysin [40, 41], matrix metallopeptidase-9 [11] and insulin-degrading enzyme [42, 43], could be exploited to limit deleterious consequences of amyloid deposition in islets. Of note, toxicity of exogenously added hIAPP or Aβ has been shown to be mediated by toxic oligomers rather than preformed fibrils [30, 44, 45]. While our experimental design did not allow us to separate the effects of the different forms of misfolded hIAPP, the toxic effect of added hIAPP on INS-1 cells was blocked by plasmin, suggesting that the cleavage of monomeric hIAPP by plasmin not only inhibited amyloid formation but, most likely, also inhibited toxic oligomer/protofibril formation. Finally, although we feel this is unlikely, we cannot exclude the possibility that prevention of hIAPP fibril formation by plasmin could be due to binding of hIAPP to plasmin rather than via hIAPP cleavage by plasmin.

We tested the amyloidogenicity and cytotoxicity of plasmin-derived hIAPP fragments. As expected, hIAPP 1–11 did not aggregate and was not toxic to INS-1 cells. When compared with full-length hIAPP, hIAPP 12–37, which contains the proposed critical amyloidogenic region for hIAPP aggregation and cytotoxicity [6], displayed accelerated aggregation kinetics. Further, we also found that the 12–37 fragment accelerates the aggregation of the full-length hIAPP, whereas the 1–11 fragment does not. The more rapid aggregation of hIAPP 12–37 likely results from multiple factors; first, we previously showed that removal of the disulfide accelerates fibril formation in the

full-length molecule [46]. Second, absence of the first 11 residues removes two of the charged residues in hIAPP, Lys-1 and Arg-11. The reduction in net charge is expected to accelerate fibril formation [47]. Third, recent cryogenic electron microscopy (cryo-EM)-based models of full-length hIAPP-derived fibrils did not define the first 10–11 residues of the polypeptide within their model(s), suggesting that these residues are not required to form the beta-sheet-rich core of the hIAPP fibrils [48–50]. Caution should be used when interpreting the lower steady-state intensity of hIAPP 12–37 in the thioflavin-T assay. The final thioflavin-T intensities in a set of kinetic assays cannot always be directly related to the amount of amyloid fibrils since they could also be due to weaker binding of the dye, the presence of fewer binding sites or a slight change in the conformation of the bound dye that reduces its fluorescence quantum yield [51]. Importantly and interestingly, irrespective of its biophysical properties, hIAPP 12–37 was not cytotoxic. Our results are in accordance with recent work that studied the effect of plasmin conjugated to quantum dots on hIAPP and reported that the resulting cleavage products are not toxic [52]. The apparent disconnect between the amyloidogenic and cytotoxic effects of hIAPP 12–37 may be explained by the fact that early aggregates of hIAPP are believed to be the major cytotoxic species, whereas fully aggregated hIAPP is inert [30]. During the amyloid fibril formation kinetics, it is well established that the lag phase represents the thermodynamically unfavourable nucleation process whereby individual monomers assemble into oligomeric species [30]. The faster aggregation of hIAPP 12–37, with no evident lag phase when aggregation was monitored using thioflavin-T, likely reduces the duration that beta cells are exposed to oligomeric species and may also lower the steady-state population of oligomers and, therefore, their cytotoxic effects. In contrast, hIAPP 12–37 accelerated aggregation of full-length hIAPP, but this did not protect INS-1 cells from hIAPP toxicity, and even appeared to increase it. In line with this observation, previous studies have reported that the serine-to-glycine substitution at position 20 (S20G) in hIAPP leads to faster aggregation than wild-type hIAPP and renders hIAPP more toxic [53, 54]. The molecular basis of these effects is not understood and these results indicate that there is still a great deal to be learned about the mechanisms by which hIAPP induces toxicity.

The cell type(s) that produce tPA within the islet under amyloid fibril-forming conditions has not been elucidated. This is of particular interest for identifying potential cellular therapeutic targets within the islet that may limit amyloid-induced beta cell toxicity. In the blood, tPA mainly derives from vascular endothelial cells [26]. Studies that have performed single-cell transcriptome profiling of human pancreatic islets have shown that tPA is expressed in human islets, predominantly in endothelial cells [55, 56]. As we recently reported that hIAPP aggregation exerts a cytotoxic and proinflammatory effect on islet endothelial cells [25], we tested whether it could also increase tPA expression in this cell type. Surprisingly, we did not find this to be the case, suggesting endothelial cells do not produce tPA in response to islet amyloid deposition. Other cell types are known to produce tPA, including immune cells [27], neurons [57] and neuroendocrine cells [58, 59]. Of note, tPA has been reported to be in rat islet delta cells [59]. hIAPP aggregation has been shown to stimulate the production of proinflammatory cytokines and chemokines from macrophages [28] and we found that it also increased tPA expression in primary BMDM. However, islet macrophage depletion did not completely prevent hIAPP aggregation-induced tPA upregulation, indicating that macrophages may not be the only cell type in the islet producing tPA under amyloidogenic conditions in vitro. Although our preliminary data suggest that an immortalised beta cell line can produce tPA in response to amyloid formation, more studies are required to confirm these findings.

In summary, we identified for the first time that the fibrinolytic system can be upregulated with hIAPP aggregation in islets and can protect beta cells from hIAPP-induced cytotoxicity. Thus, interventions aimed at increasing islet plasmin activity may reduce or limit hIAPP aggregation and, thereby, improve beta cell survival in type 2 diabetes.

References

1. Westermark P (1972) Quantitative studies on amyloid in the islets of Langerhans. Ups J Med Sci 77(2):91–94. https://doi.org/10.1517/03009734000000014

2. Hull RL, Westermark GT, Westermark P, Kahn SE (2004) Islet amyloid: a critical entity in the pathogenesis of type 2 diabetes. J Clin Endocrinol Metab 89(8):3629–3643. https://doi.org/10.1210/jc.2004-0405

3. Jurgens CA, Toukatly MN, Fligner CL et al (2011) Beta-cell loss and beta-cell apoptosis in human type 2 diabetes are related to islet amyloid deposition. Am J Pathol 178(6):2632–2640. https://doi.org/10.1016/j.ajpath.2011.02.036

4. Kahn SE, D'Alessio DA, Schwartz MW et al (1990) Evidence of cosecretion of islet amyloid polypeptide and insulin by beta-cells. Diabetes 39(5):634–638. https://doi.org/10.2337/diab.39.5.634

5. Lorenzo A, Razzaboni B, Weir GC, Yankner BA (1994) Pancreatic islet cell toxicity of amylin associated with type-2 diabetes mellitus. Nature 368(6473):756–760. https://doi.org/10.1038/368756a0

6. Westermark P, Engstrom U, Johnson KH, Westermark GT, Betsholtz C (1990) Islet amyloid polypeptide: pinpointing amino acid residues linked to amyloid fibril formation. Proc Natl Acad Sci U S A 87(13):5036–5040. https://doi.org/10.1073/pnas.87.13.5036

7. Glenner GG, Eanes ED, Wiley CA (1988) Amyloid fibrils formed from a segment of the pancreatic islet amyloid protein. Biochem Biophys Res Commun 155(2):608–614. https://doi.org/10.1016/s0006-291x(88)80538-2

8. Moriarty DF, Raleigh DP (1999) Effects of sequential proline substitutions on amyloid formation by human amylin20-29. Biochemistry 38(6):1811–1818. https://doi.org/10.1021/bi981658g

9. Hull RL, Andrikopoulos S, Verchere CB et al (2003) Increased dietary fat promotes islet amyloid formation and beta-cell secretory dysfunction in a transgenic mouse model of islet amyloid. Diabetes 52(2):372–379. https://doi.org/10.2337/diabetes.52.2.372

10. Verchere CB, D'Alessio DA, Palmiter RD et al (1996) Islet amyloid formation associated with hyperglycemia in transgenic mice with pancreatic beta cell expression of human islet amyloid polypeptide. Proc Natl Acad Sci U S A 93(8):3492–3496. https://doi.org/10.1073/pnas.93.8.3492

11. Meier DT, Tu LH, Zraika S et al (2015) Matrix metalloproteinase-9 protects islets from amyloid-induced toxicity. J Biol Chem 290(51):30475–30485. https://doi.org/10.1074/jbc.M115.676692

12. Zraika S, Hull RL, Udayasankar J et al (2007) Glucose- and time-dependence of islet amyloid formation in vitro. Biochem Biophys Res Commun 354(1):234–239. https://doi.org/10.1016/j.bbrc.2006.12.187

13. Hogan MF, Ziemann M, Harikrishnan KN et al (2019) RNA-seq-based identification of Star upregulation by islet amyloid formation. Protein Eng Des Sel 32(2):67–76. https://doi.org/10.1093/protein/gzz022

14. Astrup T, Permin PM (1947) Fibrinolysis in the animal organism. Nature 159(4046):681. https://doi.org/10.1038/159681b0

15. Nieuwenhuizen W (2001) Fibrin-mediated plasminogen activation. Ann N Y Acad Sci 936:237–246. https://doi.org/10.1111/j.1749-6632.2001.tb03512.x

16. Beringer DX, Fischer MJ, Meeldijk JD, van Donselaar EG, de Mol NJ, Kroon-Batenburg LM (2013) Tissue-type plasminogen activator binds to Aβ and AIAPP amyloid fibrils with multiple domains. Amyloid 20(2):113–121. https://doi.org/10.3109/13506129.2013.791810

17. Kranenburg O, Bouma B, Kroon-Batenburg LM et al (2002) Tissue-type plasminogen activator is a multiligand cross-beta structure receptor. Curr Biol 12(21):1833–1839. https://doi.org/10.1016/s0960-9822(02)01224-1

18. Tucker HM, Kihiko M, Caldwell JN et al (2000) The plasmin system is induced by and degrades amyloid-beta aggregates. J Neurosci 20(11):3937–3946. https://doi.org/10.1523/jneurosci.20-11-03937.2000

19. Melchor JP, Pawlak R, Strickland S (2003) The tissue plasminogen activator-plasminogen proteolytic cascade accelerates amyloid-β (Aβ) degradation and inhibits Aβ-induced neurodegeneration. J Neurosci 23(26):8867–8871. https://doi.org/10.1523/jneurosci.23-26-08867.2003

20. Jacobsen JS, Comery TA, Martone RL et al (2008) Enhanced clearance of Aβ in brain by sustaining the plasmin proteolysis cascade. Proc Natl Acad Sci U S A 105(25):8754–8759. https://doi.org/10.1073/pnas.0710823105

21. D'Alessio DA, Verchere CB, Kahn SE et al (1994) Pancreatic expression and secretion of human islet amyloid polypeptide in a transgenic mouse. Diabetes 43(12):1457–1461. https://doi.org/10.2337/diab.43.12.1457

22. Zraika S, Hull RL, Udayasankar J et al (2009) Oxidative stress is induced by islet amyloid formation and time-dependently mediates amyloid-induced beta cell apoptosis. Diabetologia 52(4):626–635. https://doi.org/10.1007/s00125-008-1255-x

23. Marek P, Woys AM, Sutton K, Zanni MT, Raleigh DP (2010) Efficient microwave-assisted synthesis of human islet amyloid polypeptide designed to facilitate the specific incorporation of labeled amino acids. Org Lett 12(21):4848–4851. https://doi.org/10.1021/ol101981b

24. Asfari M, Janjic D, Meda P, Li G, Halban PA, Wollheim CB (1992) Establishment of 2-mercaptoethanol-dependent differentiated insulin-secreting cell lines. Endocrinology 130(1):167–178. https://doi.org/10.1210/endo.130.1.1370150

25. Castillo JJ, Aplin AC, Hackney DJ et al (2022) Islet amyloid polypeptide aggregation exerts cytotoxic and proinflammatory effects on the islet vasculature in mice. Diabetologia 65(10):1687–1700. https://doi.org/10.1007/s00125-022-05756-9

26. Levin EG (1983) Latent tissue plasminogen activator produced by human endothelial cells in culture: evidence for an enzyme-inhibitor complex. Proc Natl Acad Sci U S A 80(22):6804–6808. https://doi.org/10.1073/pnas.80.22.6804

27. Hart PH, Vitti GF, Burgess DR, Singleton DK, Hamilton JA (1989) Human monocytes can produce tissue-type plasminogen activator. J Exp Med 169(4):1509–1514. https://doi.org/10.1084/jem.169.4.1509

28. Masters SL, Dunne A, Subramanian SL et al (2010) Activation of the NLRP3 inflammasome by islet amyloid polypeptide provides a

nol 11(10):897–904. https://doi.org/10.1038/ni.1935

29. Westwell-Roper CY, Ehses JA, Verchere CB (2014) Resident macrophages mediate islet amyloid polypeptide-induced islet IL-1β production and β-cell dysfunction. Diabetes 63(5):1698–1711. https://doi.org/10.2337/db13-0863

30. Zraika S, Hull RL, Verchere CB et al (2010) Toxic oligomers and islet beta cell death: guilty by association or convicted by circumstantial evidence? Diabetologia 53(6):1046–1056. https://doi.org/10.1007/s00125-010-1671-6

31. Scrocchi LA, Chen Y, Waschuk S et al (2002) Design of peptide-based inhibitors of human islet amyloid polypeptide fibrillogenesis. J Mol Biol 318(3):697–706. https://doi.org/10.1016/s0022-2836(02)00164-x

32. Wong AG, Wu C, Hannaberry E, Watson MD, Shea JE, Raleigh DP (2016) Analysis of the amyloidogenic potential of pufferfish (Takifugu rubripes) islet amyloid polypeptide highlights the limitations of thioflavin-T assays and the difficulties in defining amyloidogenicity. Biochemistry 55(3):510–518. https://doi.org/10.1021/acs.biochem.5b01107

33. Wilson HM, Haites NE, Reid FJ, Booth NA (1996) Interleukin-1 beta up-regulates the plasminogen activator/plasmin system in human mesangial cells. Kidney Int 49(4):1097–1104. https://doi.org/10.1038/ki.1996.159

34. Schrimpe-Rutledge AC, Fontès G, Gritsenko MA et al (2012) Discovery of novel glucose-regulated proteins in isolated human pancreatic islets using LC-MS/MS-based proteomics. J Proteome Res 11(7):3520–3532. https://doi.org/10.1021/pr3002996

35. Festa A, D'Agostino R Jr, Tracy RP, Haffner SM (2002) Elevated levels of acute-phase proteins and plasminogen activator inhibitor-1 predict the development of type 2 diabetes: the insulin resistance atherosclerosis study. Diabetes 51(4):1131–1137. https://doi.org/10.2337/diabetes.51.4.1131

36. Aso Y, Wakabayashi S, Yamamoto R, Matsutomo R, Takebayashi K, Inukai T (2005) Metabolic syndrome accompanied by hypercholesterolemia is strongly associated with proinflammatory state and impairment of fibrinolysis in patients with type 2 diabetes: synergistic effects of plasminogen activator inhibitor-1 and thrombin-activatable fibrinolysis inhibitor. Diabetes Care 28(9):2211–2216. https://doi.org/10.2337/diacare.28.9.2211

37. Festa A, Williams K, Tracy RP, Wagenknecht LE, Haffner SM (2006) Progression of plasminogen activator inhibitor-1 and fibrinogen levels in relation to incident type 2 diabetes. Circulation 113(14):1753–1759. https://doi.org/10.1161/circulationaha.106.616177

38. Landin K, Stigendal L, Eriksson E et al (1990) Abdominal obesity is associated with an impaired fibrinolytic activity and elevated plasminogen activator inhibitor-1. Metabolism 39(10):1044–1048. https://doi.org/10.1016/0026-0495(90)90164-8

39. Rawlings ND, Barrett AJ, Thomas PD, Huang X, Bateman A, Finn RD (2018) The MEROPS database of proteolytic enzymes, their substrates and inhibitors in 2017 and a comparison with peptidases in the PANTHER database. Nucleic Acids Res 46(D1):D624–D632. https://doi.org/10.1093/nar/gkx1134

40. Guan H, Chow KM, Shah R, Rhodes CJ, Hersh LB (2012) Degradation of islet amyloid polypeptide by neprilysin. Diabetologia 55(11):2989–2998. https://doi.org/10.1007/s00125-012-2678-y

41. Zraika S, Aston-Mourney K, Marek P et al (2010) Neprilysin impedes islet amyloid formation by inhibition of fibril formation rather than peptide degradation. J Biol Chem 285(24):18177–18183. https://doi.org/10.1074/jbc.M109.082032

42. Bennett RG, Duckworth WC, Hamel FG (2000) Degradation of amylin by insulin-degrading enzyme. J Biol Chem 275(47):36621–36625. https://doi.org/10.1074/jbc.M0061 70200

43. Hogan MF, Meier DT, Zraika S et al (2016) Inhibition of insulin-degrading enzyme does not increase islet amyloid deposition in vitro. Endocrinology 157(9):3462–3468. https://doi.org/10.1210/en.2016-1410

44. Lambert MP, Barlow AK, Chromy BA et al (1998) Diffusible, nonfibrillar ligands derived from Aβ$_{1-42}$ are potent central nervous system neurotoxins. Proc Natl Acad Sci U S A 95(11):6448–6453. https://doi.org/10.1073/pnas.95.11.6448

45. Janson J, Ashley RH, Harrison D, McIntyre S, Butler PC (1999) The mechanism of islet amyloid polypeptide toxicity is membrane disruption by intermediate-sized toxic amyloid particles. Diabetes 48(3):491–498. https://doi.org/10.2337/diabetes.48.3.491

46. Ridgway Z, Zhang X, Wong AG, Abedini A, Schmidt AM, Raleigh DP (2018) Analysis of the role of the conserved disulfide in amyloid formation by human islet amyloid polypeptide in homogeneous and heterogeneous environments. Biochemistry 57(21):3065–3074. https://doi.org/10.1021/acs.biochem.8b00017

47. Lee KH, Zhyvoloup A, Raleigh D (2019) Amyloidogenicity and cytotoxicity of des-lys-1 human amylin provides insight into amylin self-assembly and highlights the difficulties of defining amyloidogenicity. Protein Eng Des Sel 32(2):87–93. https://doi.org/10.1093/protein/gzz036

48. Gallardo R, Iadanza MG, Xu Y et al (2020) Fibril structures of diabetes-related amylin variants reveal a basis for surface-templated assembly. Nat Struct Mol Biol 27(11):1048–1056. https://doi.org/10.1038/s41594-020-0496-3

49. Röder C, Kupreichyk T, Gremer L et al (2020) Cryo-EM structure of islet amyloid polypeptide fibrils reveals similarities with amyloid-β fibrils. Nat Struct Mol Biol 27(7):660–667. https://doi.org/10.1038/s41594-020-0442-4

50. Cao Q, Boyer DR, Sawaya MR et al (2021) Cryo-EM structures of hIAPP fibrils seeded by patient-extracted fibrils reveal new polymorphs and conserved fibril cores. Nat Struct Mol Biol 28(9):724–730. https://doi.org/10.1038/s41594-021-00646-x

51. Amdursky N, Erez Y, Huppert D (2012) Molecular rotors: what lies behind the high sensitivity of the thioflavin-T fluorescent marker. Acc Chem Res 45(9):1548–1557. https://doi.org/10.1021/ar300053p

52. Yang Y, Wang Q, Li G et al (2023) Cysteine-derived chiral carbon quantum dots: a fibrinolytic activity regulator for plasmin to target the human islet amyloid polypeptide for type 2 diabetes mellitus. ACS Appl Mater Interfaces 15(2):2617–2629. https://doi.org/10.1021/acsami.2c17975

53. Cao P, Tu LH, Abedini A et al (2012) Sensitivity of amyloid formation by human islet amyloid polypeptide to mutations at residue 20. J Mol Biol 421(2–3):282–295. https://doi.org/10.1016/j.jmb.2011.12.032

54. Meier DT, Entrup L, Templin AT et al (2016) The S20G substitution in hIAPP is more amyloidogenic and cytotoxic than wild-type hIAPP in mouse islets. Diabetologia 59(10):2166–2171. https://doi.org/10.1007/s00125-016-4045-x

55. Segerstolpe Å, Palasantza A, Eliasson P et al (2016) Single-cell transcriptome profiling of human pancreatic islets in health and type 2 diabetes. Cell Metab 24(4):593–607. https://doi.org/10.1016/j.cmet.2016.08.020

56. Mawla AM, Huising MO (2019) Navigating the depths and avoiding the shallows of pancreatic islet cell transcriptomes. Diabetes 68(7):1380–1393. https://doi.org/10.2337/dbi18-0019

57. Tsirka SE, Rogove AD, Bugge TH, Degen JL, Strickland S (1997) An extracellular proteolytic cascade promotes neuronal degeneration in the mouse hippocampus. J Neurosci

17(2):543–552. https://doi.org/10.1523/jneurosci.17-02-00543.1997

58. Parmer RJ, Mahata M, Mahata S, Sebald MT, O'Connor DT, Miles LA (1997) Tissue plasminogen activator (t-PA) is targeted to the regulated secretory pathway. Catecholamine storage vesicles as a reservoir for the rapid release of t-PA. J Biol Chem 272(3):1976–1982. https://doi.org/10.1074/jbc.272.3.1976

59. Kristensen P, Nielsen JH, Larsson LI, Danø K (1987) Tissue-type plasminogen activator in somatostatin cells of rat pancreas and hypothalamus. Endocrinology 121(6):2238–2244. https://doi.org/10.1210/endo-121-6-2238

Authors and Affiliations

Nathalie Esser[1,2,3,4] · Meghan F. Hogan[1,2] · Andrew T. Templin[1,2,5] · Rehana Akter[1,2] · Brendy S. Fountaine[1] · Joseph J. Castillo[1,2] · Assam El-Osta[6] · Lakshan Manathunga[7,8] · Alexander Zhyvoloup[9] · Daniel P. Raleigh[7,8,9] · Sakeneh Zraika[1,2] · Rebecca L. Hull[1,2] · Steven E. Kahn[1,2]

✉ Daniel P. Raleigh
d.raleigh@ucl.ac.uk

✉ Steven E. Kahn
skahn@uw.edu

1 Veterans Affairs Puget Sound Health Care System, Seattle, WA, USA

2 Division of Metabolism, Endocrinology and Nutrition, Department of Medicine, University of Washington, Seattle, WA, USA

3 Laboratory of Immunometabolism and Nutrition, GIGA, University of Liège, CHU of Liège, Liège, Belgium

4 Division of Diabetes, Nutrition and Metabolic Disorders, Department of Medicine, CHU of Liège, Liège, Belgium

5 Division of Endocrinology, Department of Medicine, Roudebush VA Medical Center and Indiana University School of Medicine, Indianapolis, IN, USA

6 Epigenetics in Human Health and Disease Program, Baker Heart and Diabetes Institute, Melbourne, VIC, Australia

7 Department of Chemistry, Stony Brook University, Stony Brook, NY, USA

8 Laufer Center for Physical and Quantitative Biology, Stony Brook University, Stony Brook, NY, USA

9 Research Department of Structural and Molecular Biology, University College London, London, UK